Evaluating the performance of gravity-driven membrane filtration as desalination pretreatment of shale gas flowback and produced water

Revised manuscript for ***Journal of Membrane Science***

Date: 2019-05-29

Evaluating the performance of gravity-driven membrane filtration as desalination pretreatment of shale gas flowback and produced water

Haiqing Chang[a,b], Baicang Liu[a,b,*] Huizhong Wang[a], Si-Yu Zhang[c], Sheng Chen[d], Alberto Tiraferri[e], Yueqin Tang[a]

[a] College of Architecture and Environment, Sichuan University, Chengdu 610207, PR China

[b] Institute of New Energy and Low Carbon Technology, Sichuan University, Chengdu 610207, PR China

[c] School of Civil and Environmental Engineering, Georgia Institute of Technology, Atlanta, GA 30332, USA

[d] College of Light Industry, Textile and Food Engineering, Sichuan University, Chengdu 610065, PR China

[e] Department of Environment, Land and Infrastructure Engineering, Politecnico di Torino, Corso Duca degli Abruzzi 24, 10129 Turin, Italy

[*] Corresponding author (Baicang Liu).

Tel.: + 86 28 85995998; fax: +86 28 62138325.

E-mail address: bcliu@scu.edu.cn.

ABSTRACT

The shale gas extraction industry generates a large quantity of highly contaminated flowback and produced water (FPW), with great impacts on human health and the environment. In this study, gravity-driven membrane (GDM) filtration was evaluated over a 612-day period as a pre-treatment of FPW for its subsequent desalination. The various investigated GDM systems showed similar contaminant removal, and their steady-state fluxes (i.e., 0.65-0.82 L/($m^2 \cdot h$)) were not significantly correlated to membrane configurations or to the hydrostatic pressures. The flux decline was primarily due to a reversible resistance, which accounted for a large proportion (>89%) of the total hydraulic resistance. Compared to traditional ultrafiltration, the GDM pretreatment resulted in better desalination performance for the subsequent nanofiltration or reverse osmosis step, which were characterized by higher organic removal and generally higher permeate fluxes. More than 60 bacterial genera and 8 eukaryotic genera were detected in the shale gas FPW, with the kingdoms *Alveolata* and *Stramenopiles* (within the eukaryote domains) reported for the first time. The biofouling layer of GDMs had a lower bacterial diversity but a higher eukaryotic diversity than the FPW feed water. The eukaryotic community, including *Alveolata*, *Fungi*, *Stramenopiles* and *Metazoa*, played a major role in the flux behavior.

Key words: shale gas; flowback and produced water (FPW); gravity-driven membrane (GDM); desalination pretreatment; microbial community

1. Introduction

Shale gas is one of the most rapidly expanding resources in the oil and gas exploration industry, but its extraction is associated with severe environmental problems, including significant freshwater consumption and the complex management of shale gas flowback wastewater. Large volumes of flowback and produced water (FPW) (~ 5,200-25,870 m^3 per horizontal well) are typically generated during shale gas extraction [1]. Based on the prediction of shale gas drilling rates in the Haynesville shale (U.S.) and in the Sichuan Basin shale (China), the number of drilling wells will reach a maximum in the next several years [2]. Therefore, the amount of FPW will also reach a peak value and its management is an urgent issue to guarantee favorable economics of shale gas extraction, while protecting human health and environmental resources [3,4]. The situation is complicated by the numerous types of contaminants that have been detected in shale gas FPW and that pose great challenges for the reuse or discharge of these wastewaters [5,6].

Several desalination technologies, including reverse osmosis (RO), nanofiltration (NF), forward osmosis, and membrane distillation have been proposed to deal with shale gas FPW, for their reuse or surface water discharge [6-8]. Effective pretreatment is a critical factor influencing the sustainable operation of these desalination processes, and it can be accomplished using low-pressure membrane (i.e., ultrafiltration (UF) and microfiltration (MF)) [6,9]. Nevertheless, the appeal of UF pretreatment is limited by its relatively high energy consumption due to operational costs and strategies for membrane fouling mitigation; in contrast, the recently developed gravity-driven membrane (GDM) filtration is typically more favorable than conventional UF [10]. GDM filtration has received increasing attention in decentralized water treatment due to its advantages, which include ultra-low hydrostatic pressure (e.g., with height of 0.4-1.0 m) and no need for backwashing [11]; therefore, GDM may be attractive also for FPW.

The application of GDM has recently extended from surface water [12] to other sources, including rainwater, wastewater, grey water, and seawater [10]. As opposed to surface water as feed solution [11], the permeate flux values in the GDM filtration of seawater depended not only on the feed water properties, but also on the operating temperature and the hydrostatic pressure [13,14]. With respect to membrane properties, UF membranes rather than MF membranes [14-16] have been usually adopted in GDM systems, with flat sheet membranes a more common configuration than hollow fiber membranes [14,15,17,18]. Together with feed organics and operation conditions, another critical factor affecting the flux stabilization and the general flux behavior during GDM filtration is the composition of the biofouling layer [11,12,19,20].

Understanding the nature and the proportion of different microorganisms in the FPW is important to predict the performance of the system and to design suitable mitigation strategies. Despite of high salinities and concentrations of biocides [21] in usual shale gas FPW, more than one-third of the organic substances contained in the FPW are biodegradable, showing the potential of biological treatment in FPW treatment [22]. The presence of microorganisms in shale gas FPW causes concern for the safety and performance of the operation, and reports on the compositions of the microbial community have recently increased [23-30]. Published research showed that microorganisms may play a great role in organic removals from shale gas FPW using biological treatment processes, such as biologically-active filtration [8] and sequencing batch reactor-membrane bioreactor process [31]. Based on these previous results, GDM is expected to perform well as desalination pretreatment. However, the compositions and changes of microbial community during GDM filtration of shale gas FPW, as well as the impacts of microorganisms on removals of contaminants, need to be investigated.

The composition of shale gas FPW is associated to the complexity of its treatment, compared to more conventional municipal wastewater or other produced water [32], also because FPW water exhibits significant spatial and temporal change [6]. This study aims at evaluating the applicability and performance of GDM as a pretreatment for desalinating shale gas FPW from the Sichuan Basin. Specifically, the objectives of this work are: (a) to examine the influence of hydrostatic pressure and membrane configuration on steady-state flux and hydraulic resistance; (b) to assess the removal behavior of contaminants from shale gas FPW by GDM filtration; (c) to analyze the microbial community composition of the raw shale gas FPW and of the biofouling layer of GDM; (d) to determine the effects of GDM on the desalination performance of NF and RO processes; and (e) to investigate the changes in the performance of the membranes after long-term exposure to shale gas FPW.

2. Materials and methods

2.1. Shale gas FPW and water quality analysis

The shale gas wastewater was collected from a storage tank in Longhui Town, Weiyuan County in the Sichuan Basin, China on December 14, 2016. The storage tank with an effective volume of 10,000 m^3 received untreated FPW from horizontal shale gas wells. The samples were collected from mid depth (about 1.5 m below the surface) of the storage tank. The primary water parameters of the raw FPW were summarized previously [33,34]. The permeates from GDM systems were collected every 2-3 weeks for water quality analysis. Total dissolved solid (TDS) and electrical conductivity (EC) were measured by an Ultrameter II 6PFC portable multifunctional meter (Myron L Company, Carlsbad, CA, USA). Temperature and pH were measured by using a mercury thermometer and a pH meter (PB-10, Sartorius Scientific Instruments Co., Ltd., Gottingen, Germany), respectively. Turbidity and alkalinity were determined by a turbidimeter (TL2310, Hach Company, Loveland, USA) and by acid-base indicator titration method, respectively. A UV-Vis spectrophotometer (Orion AquaMate 8000, Thermo Fisher Scientific Inc., MA, USA) was employed to measure UV absorbance at 254 nm (UV_{254}). The chemical oxygen demand (COD) and dissolved organic carbon (DOC) were monitored using the fast digestion-spectrophotometric method with a 5B-1F(V8) fast digestion meter (Lianhua Environmental Protection Technology Co., Ltd., Lanzhou, China) and an automatic total organic carbon analyzer (TOC-L, Shimadzu, Japan), respectively. The 15-min silt density index (SDI_{15}) of the GDM permeate and UF permeate were measured as described in detail in ASTM D4189-07 (2014) [35].

2.2. UF membranes and GDM setup

Two types of commercially available polyvinylidene fluoride (PVDF) UF membranes with different configurations (i.e., hollow fiber and flat sheet) were employed. Outside-in hollow fiber membranes and flat sheet UF membranes were obtained from Litree Purifying Technology Co., Ltd. (Haikou, China) and Tianchuang Waterpure Equipment Co., Ltd (Hangzhou, China), respectively. The two UF membranes had the same nominal molecular weight cut-off of 100 kDa. Each hollow fiber membrane had a single fiber with an outer diameter of 1.8 mm and a length of 18 cm, thus, the active filtration area of each hollow fiber membrane was roughly 10 cm^2. The flat sheet UF membrane was round with a diameter of 23 mm, resulting in an effective filtration area of 4.15 cm^2. The normalized pure water permeability coefficients (at 20 $^{\circ}C$) of hollow fiber and flat sheet membranes were 3.5 and 22.4 L $m^{-2}h^{-1}kPa^{-1}$ (350 and 2240 L $m^{-2}h^{-1}bar^{-1}$). Detailed information about surface physicochemical characteristics of both membranes could be found in our previous study [36].

The GDM setup consisted of a raw water tank, a constant-level water tank, and several customized GDM filtration cells, as presented in Fig. S1 (Supporting Information). GDM systems comprising either hollow fiber membranes or flat sheet membranes were deployed for 612 days using the raw FPW as feed solution to evaluate the impact of membrane configuration, using the same pressure head of 0.8 m for the two configurations. Starting from the 100^{th} day of investigation, GDM experiments were also run for 512 days using hollow fiber membranes under different hydrostatic pressures of 40, 120, and 160 mbar (i.e., pressure head, H = 0.4, 1.2, and 1.6 m). As opposed to the most common configurations of GDM systems [10], in this work the permeate outlet of the module was connected to an overflow tank using a hose with full pipe flow and with submerged discharge. According to Bernoulli's equation [37], the driving force of each GDM test was the water head difference between the water level in each tank and the permeate outlet of the system into the overflow tank (Fig. S2, Supporting Information), with the detailed calculation summarized in Section SI1 [38-40]. The systems were operated continuously at water temperatures in the range 15-30 °C (Fig. S3, Supporting Information).

2.3. Membrane flux and hydraulic resistance

The permeate flux (L $m^{-2}h^{-1}$, LMH) observed during GDM experiments was normalized to that measured at 20 °C to eliminate the influence of temperature, using Eq. (1):

$$J_{20} = (J_T \cdot \mu_T)/\mu_{20} \quad (1)$$

where J_{20} (LMH) and J_T (LMH) represent the corrected permeate flux at 20 °C and the measured permeate flux at the prevailing temperature T (°C), respectively; μ_{20} (Pa·s) and μ_T (Pa·s) are the water viscosities at 20 °C and at the prevailing temperature T, respectively. μ_T (cP, 1 cP = 10^{-3} Pa·s) was calculated with an empirical relationship [41]:

$$\mu_T = 1.784 - (0.0575 \cdot T) + (0.0011 \cdot T^2) - (10^{-5} \cdot T^3) \quad (2)$$

The total hydraulic resistance (R_{total}, m^{-1}) was calculated based on Darcy's law:

$$R_{total} = TMP/(\mu_T \cdot J_T) \quad (3)$$

where TMP is the transmembrane pressure (i.e., hydrostatic pressure head, or height)

(Pa). The intrinsic membrane resistance (R_{mem}) was measured using ultrapure water before the FPW was fed into the system. The reversibility of membrane fouling is expressed by the percentage of reversible resistance (R_{rev}) over the total hydraulic resistance (R_{total}). The reversible fouling resistance (i.e., biofouling layer resistance) can be obtained by subtracting the clean membrane resistance (R_{mem}) and the irreversible fouling resistance (R_{irr}) from the total hydraulic resistance (R_{total}).

$$R_{total} = R_{mem} + R_{rev} + R_{irr} \quad (4)$$

At the end of operation, the biofouling layer was firstly detached from membrane surface by forward flushing with 100 mL of ultrapure water using a syringe. Then, the cleaned membrane was returned to the GDM system to determine the permeate flux by filtering again the raw FPW. It is assumed that the resistance after flushing was the sum of R_{irr} and R_{mem} [42].

2.4. Scanning electron microscopy (*SEM*) *observation*

The membrane samples were used for contact angle measurements and for SEM observation after drying under ambient conditions. The membrane surface morphology was determined with a SU8200 SEM (Hitachi, Japan) after gold-coating by a magnetron ion sputter metal coater device (MSP-2S, IXRF Systems, Inc., Japan), while the cross-section of membrane samples was observed with a SU3500 SEM (Hitachi, Japan) after coating with a sputter coater (Q150R ES, Quorum, UK).

2.5. Microbial community analysis

To explore the reason for flux decline and stabilization in the GDM systems, the biofouling layers of hollow fiber and flat sheet membranes were carefully removed at the end of the experiment for analysis of the microbial community. Meanwhile, the microbial community of the raw shale gas FPW was also analyzed. Genomic DNA (gDNA) of the microbial community in biofouling layer samples and sludge of raw shale gas FPW was extracted, based on the reported method [43]. The purity and the concentration of each DNA sample were measured by a NanoDrop2000 UV-vis spectrophotometer (Thermo Scientific, Wilmington, USA) at wavelengths of 260 nm and 280 nm, respectively. A DYY-6C agarose gel electrophoresis (Beijing Liuyi Biotechnology Co., Ltd., China) was used to determine the integration of the DNA samples. After this step, the 16S rRNA and 18S rRNA genes were amplified by quantitative polymerase chain reaction (PCR) using a GeneAmp® 9700 PCR thermocycler (Applied Biosystems, Foster City, CA, USA) in a 20 μL volume reaction. The universal primer sets 338F (5'-ACTCCTACGGGAGGCAGCAG-3') and 806R (5'-GGACTACHVGGGTWTCTAAT-3') [44] were used to amplify the hypervariable region V3-V4 of the bacterial 16S rRNA genes. The eukaryotic 18S rRNA genes were amplified using primer pairs SSU0817F (TTAGCATGGAATAATRRAATAGGA) and 1196R (TCTGGACCTGGTGAGTTTCC). The detailed description of the composition of the PCR reaction mixture, the amplification conditions, as well as of the Illumina MiSeq sequencing and sequencing data processing are summarized in Section SI6 (Supporting Information).

Usearch software (version 7.1, http://drive5.com/uparse/) was used to group sequences with ≥ 97% (similarity) identity into operational taxonomic units (OTUs). The analyses of microbial community composition, the alpha diversity (e.g., Chao, Shannon, Simpson, ACE, and Coverage) and the beta diversity (i.e., Bray-Curtis distance and Non-Metric Multidimensional Scaling (NMDS)) were performed using the free online Majorbio I-Sanger Cloud Platform (www.i-sanger.com). A Bray-Curtis distance matrix was plotted in a 2-dimensional NMDS ordination, where distance between samples represents their dissimilarity. Sequences were deposited in the NCBI Short Read Archive under Bioproject accession number PRJNA508877, with biosample numbers SAMN10532262–SAMN10532264 (for 16S rRNA genes) and SAMN10532265–SAMN10532267 (for 18S rRNA genes).

2.6. Desalination setup using NF or RO

Bench-scale tests using NF or RO membranes were carried out to verify the positive influence of GDM pretreatment on the subsequent desalination performance. NF and RO membranes were chosen because they were appropriate desalination strategies for the FPW in Sichuan Basin shale gas operation [33,34] due to its low TDS concentration. The permeate stream from the GDM systems was batch-fed to a NF or RO unit. As a comparison, the permeate stream from a traditional UF process was also used as feed water of the desalination processes. Similar to the hollow fiber UF membrane in GDM (Section 2.2), a hollow fiber membrane module (with effective area of 10 cm^2) was employed for the traditional UF process. Both GDM filtration and traditional UF process were fed with the same raw shale gas FPW, but the traditional UF process was operated under constant flux mode (with a flux of 50 LMH), as described in a previous study [33]. The NF and RO composite membranes had an active layer of aromatic polyamide and were provided by Vontron Membrane Technology Co., Ltd. (Guiyang, China). The effective filtration area of NF or RO membrane was 14.6 cm^2. The NF/RO setup is also illustrated in Fig. S1 (Supporting Information), with membrane properties described in detail in previous studies [33,34]. The NF or RO test was performed using a dead-end stirred cell (HP 4750, Sterlitech Corp., Kent, USA) at a stirring speed of 200 r/min. Each NF membrane was operated at an applied pressure of 2.0 MPa (20 bar), and it was terminated when a water recovery of 70% was obtained. The RO test was carried out at an applied pressure of 5.0 MPa (50 bar) with a final water recovery of 50%.

3. Results and discussion

3.1. Behavior of the permeate flux

Fig. 1 illustrates the trend of the permeate flux (normalized to 20 °C) and the fouling resistance of UF membranes in the GDM systems. As presented in Fig. 1a, the permeate flux using flat sheet membrane declined rapidly due to biofouling from 179 to 8.5 LMH during the first week. After this period, the flux decreased very slowly, reaching a near steady-state flux value of 0.65±0.08 LMH after roughly 300 days of operation. The flux of the hollow fiber UF membranes under the same pressure head of H = 0.8 m was initially lower than that observed with flat sheet membranes, consistent with a lower water permeance, but it was also characterized by a rapid decline during the first few weeks of operation, reaching values of 3.0 and 2.0 LMH after 5 and 8 weeks, respectively. The near steady-state value was 0.71±0.10 LMH, observed near the end of the experiment. Therefore, in this study the steady-state flux was not significantly influenced by membrane configuration, orientation, or intrinsic water permeability coefficient (p > 0.05). Flux differences due to the membrane configuration were reported in previous studies [14-17].

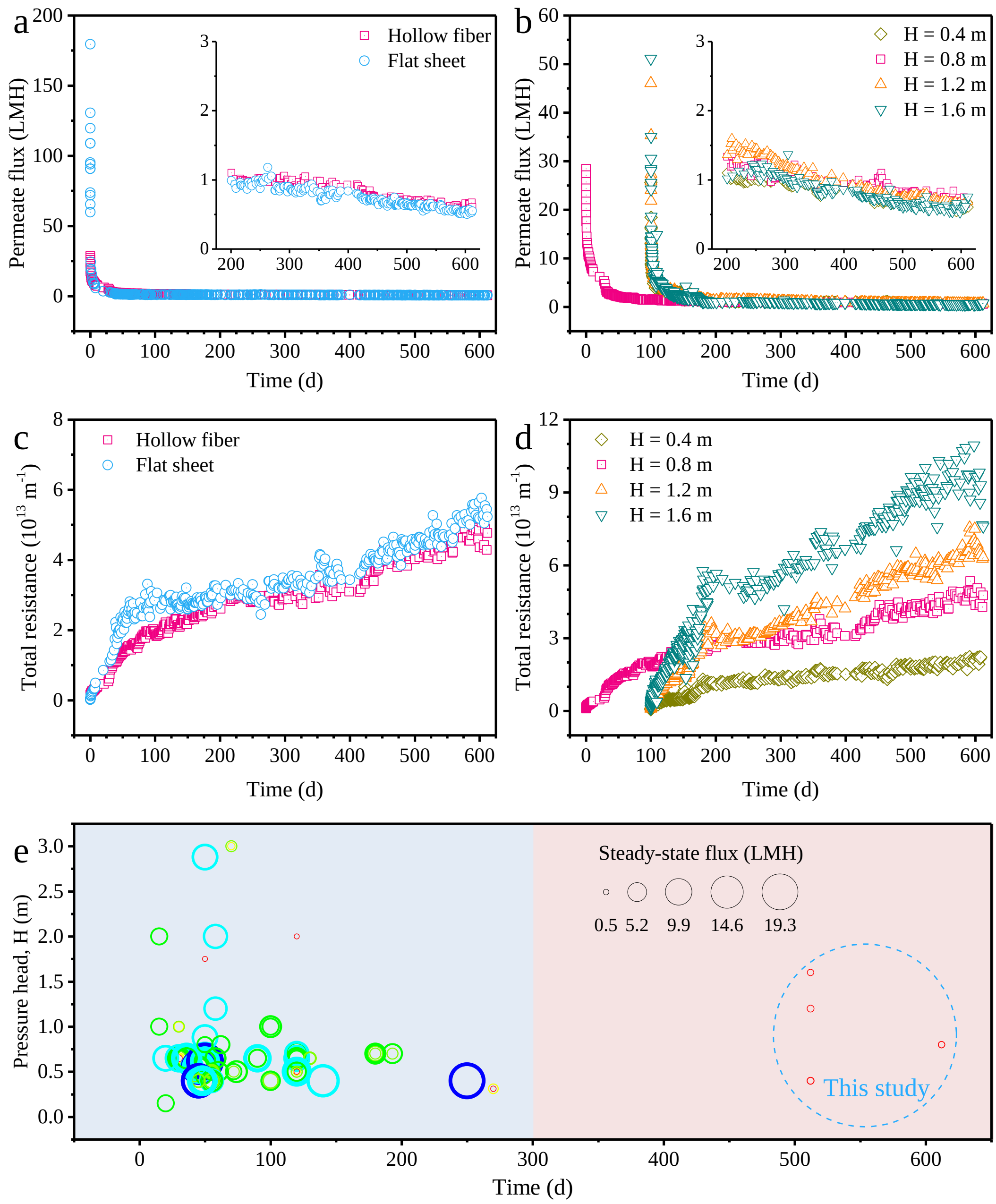

Fig. 1. Permeate flux and filtration resistance behavior. Variation of (a)(b) normalized permeate flux and (c)(d) filtration resistance of GDMs during long-term operation: (a)(c) pressure head, H = 0.8 m, and (b)(d) different hydrostatic pressures for hollow fiber

membranes; (e) comparison of the steady-state flux of GDMs in this study and in published literature. Detailed information about the steady-state fluxes of GDM systems in published literature are summarized in Table S1 of the Supporting Information.

The same flux decline and stabilization trend was observed for hollow fiber membranes under different pressure heads (Fig. 1b). The steady-state values (usually reached after roughly one year of operation) were 0.82±0.10, 0.75±0.09, and 0.69±0.09 LMH for GDMs under pressure heads, H, of 0.4, 1.2 and 1.6 m, respectively. Therefore, the influence of hydrostatic pressure (i.e., height) on steady-state flux values was also not significant, consistent with trends previously reported for the GDM filtration of rain or river water [17,45]. However, the steady-state flux values presented here were lower than those reported by several previous investigations, as summarized in Fig. 1e. This difference is rationalized with the larger pollutant concentrations (e.g., salinity and organics) of the shale gas FPW investigated in this study and with an overall longer operation time (Fig. 1e and Table S1), suggesting that GDM systems should be run for long periods to observe a complete flux behavior.

Published studies involving GDM filtration revealed that the predation of eukaryotic microorganisms resulted in the formation of a heterogeneous structure in the biofouling layer, responsible for the observed rapid decline and long-term stabilization of the permeate flux [12,46]. The fouling behavior can also be described in terms of hydraulic resistance. The sharp decrease in the permeate flux of the flat sheet membrane system in the first days of operation led to higher hydraulic resistances compared to hollow fiber membranes in this initial period, but similar resistances were achieved at larger time values (Fig. 1c). As shown in Fig. 1d, the GDM at a pressure head of 0.4 m resulted in the lowest resistance among the systems operated with different pressure heads, with a value of 2.1×10^{13} m^{-1} at the end of the test. This value was comparable to that observed during GDM filtration of grey water after 120 days [42,47]. Because the observed steady-state fluxes were comparable for the different pressure heads (Fig. 1b), based on Eq. (3) higher hydraulic resistances were associated with increased hydrostatic pressures (Fig. 1d).

3.2. Membrane fouling reversibility during GDM filtration

Fig. 2 summarizes the results on fouling reversibility of GDMs in shale gas FPW treatment. Regarding membrane configuration (Fig. 2a), near complete recovery of the baseline resistances were observed via hydraulic cleaning for both hollow fiber and flat sheet membranes (96.1% and 98.9%). Moreover, regardless of the value of the pressure head, the dominant reason for flux decline was always the hydraulically reversible resistance, which accounted for a large proportion of the total hydraulic resistance (89.6-97.7%), with increased proportion as the hydrostatic pressures increased (Fig. 2b). These values are consistent with the GDM filtration of grey water, sewage or rain water, reported previously [18,42,47-49]. The results suggest the possibility to effectively recover the flux of GDMs by simple physical cleaning after long-term operation.

The GDMs in the two configurations and employed under the same pressure head

(0.8 m) were analyzed using SEM after the filtration (612 days) and cleaning steps. While large amounts of deposited foulants was observed on the surface of the membranes following filtration (Fig. 2c), their efficient removal after physical flushing was confirmed by the micrographs. The thickness of the fouling layer on the flat-sheet membrane (~5.5 μm) was higher than that on the hollow fiber membrane (~4.1 μm), probably due to the different orientation (horizontal versus vertical). Note that these thicknesses were tested in this study after membrane drying, which may have led to shrinkage. This is possibly the reason why the thicknesses reported in this study were smaller than those observed previously after GDM filtration of surface water [11,12,19,20,38,46], grey water [42,47], rain water [49], or seawater [13-15], while they were similar with that obtained after drying the membranes used for the GDM filtration of sewage [48].

The surface contact angle of water may also be used as a proxy to evaluate the fouling reversibility and these results are presented in Fig. S4 of the Supporting Information. The wettability of the hollow fiber membranes increased significantly after filtration (the contact angle decreased), likely due to the deposition of hydrophilic organic foulants [50]. Following cleaning, the contact angles increased slightly but did not reach the value measured with pristine samples, suggesting that while most of the cake layer was removed, some irreversibly deposited substances were still present on the membrane surface, which did not affect significantly the permeate flux.

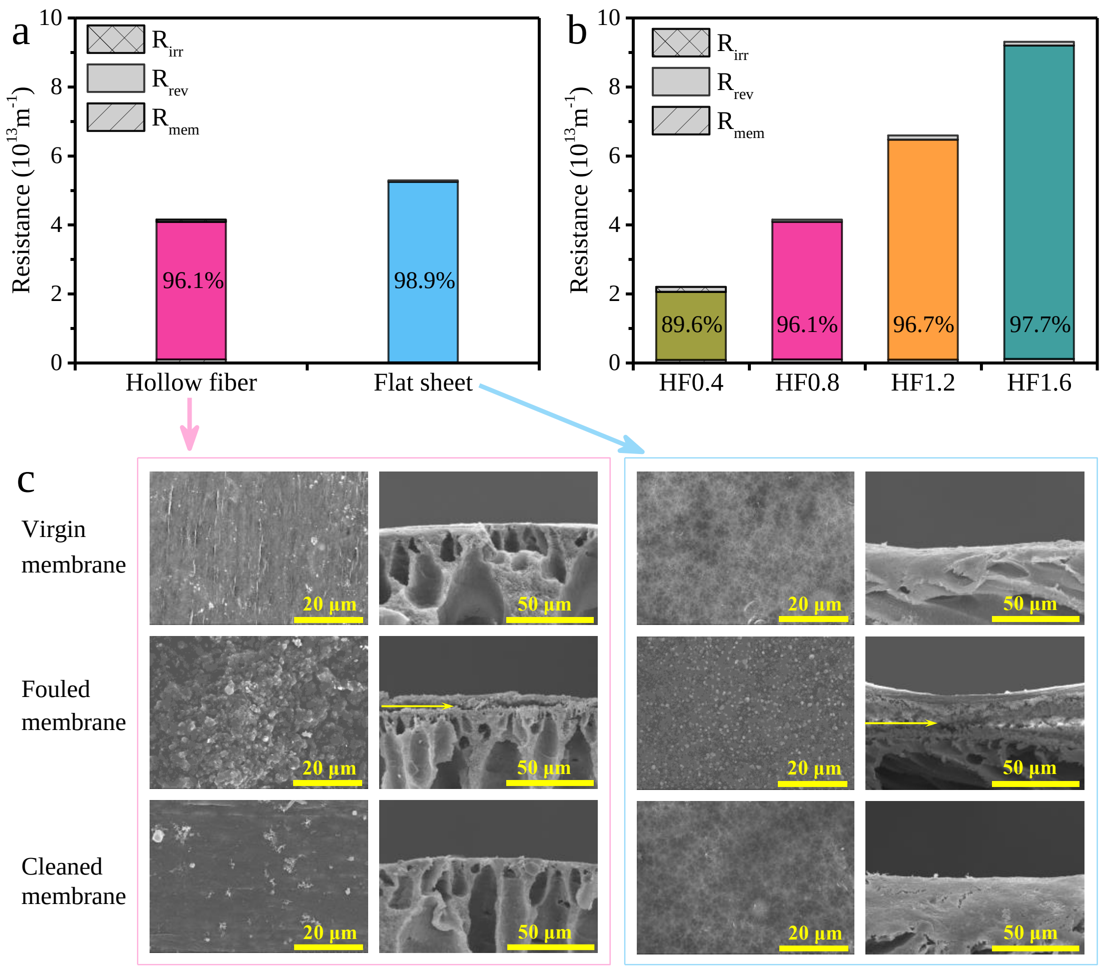

Fig. 2. Fouling reversibility of the UF membranes. Filtration resistances (a)(b) in different GDM systems; surface and cross-sectional SEM micrographs (c) of the virgin, fouled, and cleaned membrane samples. The abbreviations, HF0.4, HF0.8, HF1.2 and HF1.6, refer to hollow fiber membranes operated under a pressure head of 0.4, 0.8, 1.2 and 1.6 m, respectively.

3.3. Pollutant removal of GDM from shale gas FPW

Fig. 3 illustrates the permeate quality and the removals of primary pollutants in GDM systems under different operational conditions. As expected, comparable concentrations of TDS or EC were observed for the feed water (raw FPW) and the permeates for all the GDM systems (Figs. 3a-b), as these compounds are not effectively removed by UF membranes [33,34]. As shown in Fig. 3c, decreased DOC concentrations were observed in GDM permeates when compared to the raw FPW, with removals in the range 11.7-20.6%. The membrane configuration or hydrostatic pressure did not significantly ($p > 0.05$) influence the DOC removal efficiencies. Similar results were observed for other organic parameters, and the average removals were 11.1-14.2% and 12.2-19.0% for COD and UV_{254}, respectively (Figs. 3d-e). The removal efficiencies were similar to those reported for the traditional UF filtration of shale gas FPW [8,33,34].

The GDM systems removed instead most of the particulate matter, with residual turbidities lower than 0.05 NTU for the permeates of all the GDMs. The turbidity removals were nearly complete (> 99.9%), as presented in Fig. 3f. With respect to alkalinity, the values in the GDM permeate samples ranged from 249 to 431 mg/L, with removals of 43.3-52.5%. The average pH of the feed water was 7.7, and slightly increased pH values (8.0-8.1) were observe for the permeate streams of GDM systems (Fig. 3h). The results presented here are noteworthy in that they suggest the suitability of GDMs for field application, thus eliminating the need for cumbersome procedures associated with traditional UF processes, such as cross-flow operation, backwashing, and chemical cleaning [10].

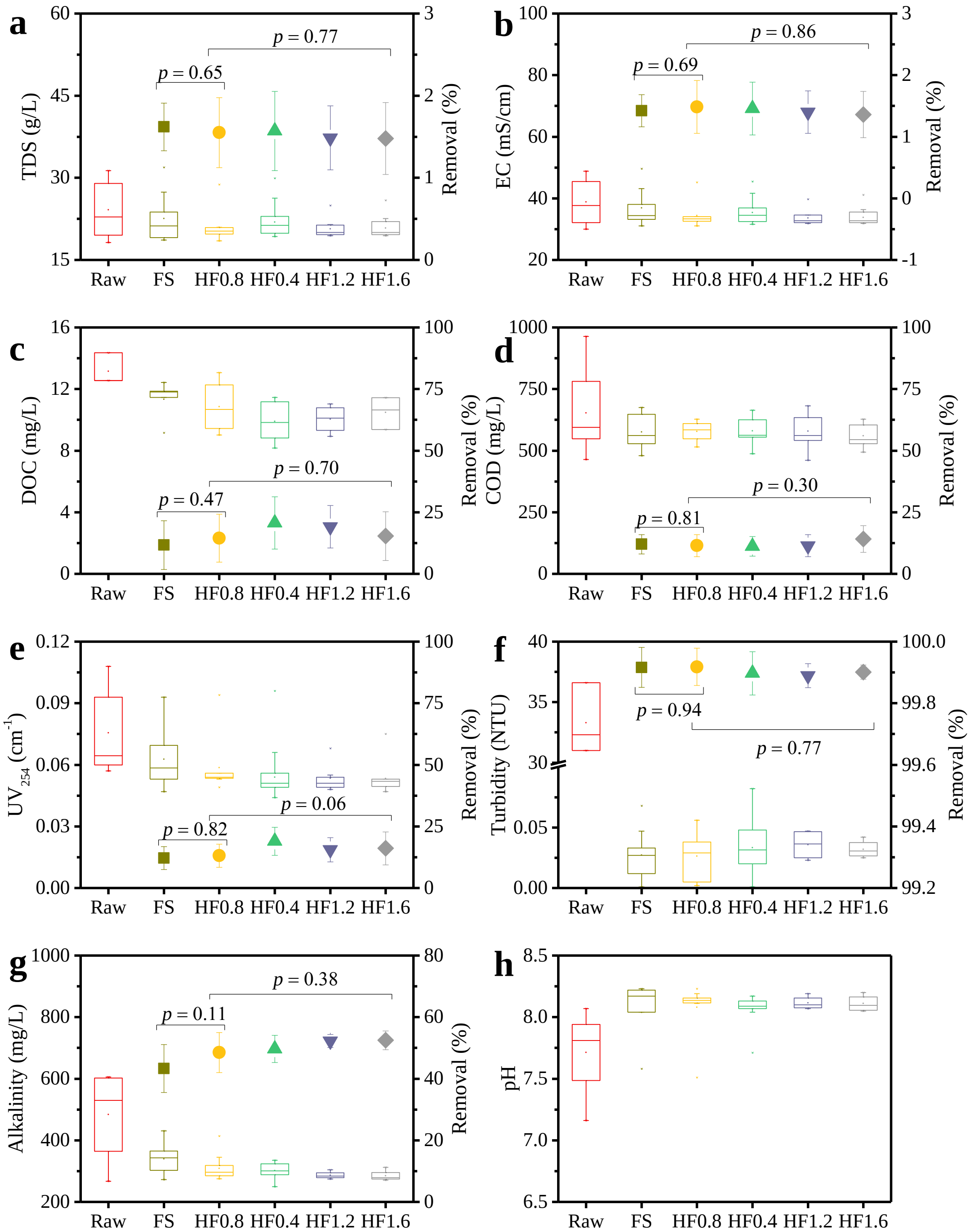

Fig. 3. Water quality and removal efficiencies of main pollutants in GDM systems. Values of (a) TDS, (b) EC, (c) DOC, (d) COD, (e) UV_{254}, (f) turbidity, (g) alkalinity and (h) pH. The box bars represent the concentrations in the raw feed and in the permeate waters, while the solid points represent the corresponding removals. The abbreviation FS refers to flat sheet membranes, while the other abbreviations are the same as in Fig. 2.

The membrane performance may be deteriorated after exposure to shale gas FPW for a long period [51]. The effects of exposure time (0, 32, 640 d) on membrane performance, including tensile strength, elongation, membrane permeability, and contact angle, are presented in Fig. S5 (Supporting Information). Tensile strength and ultimate elongation decreased for the UF membrane exposed for 32 days when compared to the pristine one, whereas the exposure duration (32 and 640 days) did not have a significant effect on these mechanical properties (Figs. S5a-b). There was no significant difference between the permeability and water contact angle of the pristine UF membrane and that of the membrane exposed for one month, but an obvious decrease in both parameters was observed for the membrane exposed for 640 days (Figs. S5c-d). These results are consistent with SEM observations, which revealed that no obvious foulants were deposited on the membrane surface after exposure for 32 days, while a 640-day exposure promoted large foulant coverage (Fig. S5e). In summary, while the membrane mechanical properties appeared to be more sensitive than other parameters to FPW exposure, their change did not lead to a deterioration of membrane filtration performance or water quality in long-term operation (Fig. 3).

3.4. Bacterial and eukaryotic community composition

The bacterial community in the raw FPW consisted of 90 OTUs (Table 1), while the observed OTUs numbers for eukaryotic community ranged between 9 and 32. Compared to the raw shale gas FPW, the observed richness (ACE, Chao) of bacterial community generally decreased in the biofouling layer of GDMs, while that of eukaryotic community increased. For bacterial community, the decrease in Shannon and increase in Simpson indices suggest that there was a slight decrease in diversity in the biofouling layer of GDMs. In contrast, for the eukaryotic community, a higher diversity of the biofouling layer compared to the raw shale gas FPW was evidenced by the increase in Shannon index and decrease in Simpson index. The estimates of community coverage obtained in this study (99.9%) suggest that the presented sequences represented the vast majority of the microbial community. The rarefaction curves (Fig. S6, Supporting Information) indicate that most of the bacteria and eukaryotes reached saturation.

Table 1 Abundance, coverage, richness, and diversity of bacterial 16S rRNA genes and eukaryotic 18S rRNA genes

Sample	No. of sequences	OUT at 97% identity	Coverage	ACE	Chao	Shannon	Simpson
16S rRNA							
FPW	55978	90	1.0000	90.0	90.0	2.86	0.15
HF membrane	48065	82	0.9998	86.6	91.3	2.24	0.21
FS membrane	36997	74	0.9998	80.7	78.7	2.09	0.26
18S rRNA							
FPW	37140	9	0.9999	30.0	12	0.01	1.00
HF membrane	34459	17	1.0000	17.7	17	0.37	0.87
FS membrane	37192	32	1.0000	32.0	32	0.74	0.73

3.4.1. Bacterial community of the biofouling layer in GDM and comparison with the raw FPW

Fig. 4 presents taxonomic compositions of bacterial communities. Ten bacterial phyla were detected in the raw shale gas FPW (Fig. 4a), accounting for half of that recovered from shale gas produced water in Sichuan Basin [29]. *Proteobacteria* (45.3%), *Planctomycetes* (38.8%) and *Bacteroidetes* (11.0%) constituted 95% of the bacteria in the raw shale gas FPW. Among these phyla, mesophiles and moderate halophiles [27], i.e., *Bacteroidetes* and *Proteobacteria*, were detected. Bacterial phyla, including *Proteobacteria*, *Planctomycetes*, *Bacteroidetes*, *Acidobacteria*, *Firmicutes* and *Lentisphaerae* [23,26,29,44,52], were also detected in other shale gas FPWs. The dominant classes in shale gas FPW in this study included *Phycisphaerae* (38.8%), *Alphaproteobacteria* (21.9%), *Gammaproteobacteria* (20.7%), and *Bacteroidetes_Incertae_Sedis* (9.8%) (Fig. 4b). The same classes were detected with high abundances in biofouling layers during GDM filtration of seawater [13,16], and comparable microbial diversity was also reported in samples from other shale gas FPWs [26,27,53-56]. At the genus level (Fig. 4c), more than 60 bacteria were recovered in the raw shale gas FPW. Among them, *SM1A02* and *Rehaibacterium* represented each approximately half of the total genera. Most of the genera, such as *SM1A02* and *Rehaibacterium*, *Filomicrobium*, *Bryobacter*, *Roseovarius*, *Methylophaga* and *Alcanivorax* in the shale gas FPW in this work, differed from those detected in Sichuan Basin shale gas produced water [29]. Nevertheless, the genera *Marinobacterium* and *Pseudomonas* have been also reported in previous studies [24,28,30]. As a matter of fact, there is a significant discrepancy between the relative abundance of bacteria (e.g., in terms of order or gene) in shale gas FPWs reported in the published literature [24,25]. This result is most likely due to the significant differences of geographic location, depth, composition of fracturing fluid, well age, and general water quality in this study compared to the previous studies [57].

An obvious divergence from raw FPW was observed in terms of dominant bacterial phyla in the GDM biofouling layer (Fig. 4a). For both the hollow fiber and the flat sheet membranes, the relative abundances of *Planctomycetes* and *Proteobacteria* decreased; however, while *Bacteroidetes* increased to 25.9% for the hollow fiber membranes, they decreased to 8.8% in the biofouling layer on flat sheet membranes. At the genera level (Fig. 4c), the proportion of *SM1A02* and *Gammaproteobacteria* increased in the biofouling layers compared to the raw FPW. Some differences of microbial community compositions between the two membrane configurations were observed. *Order_III* (*Bacteroidetes*) became a major microbe in the biofouling layer of hollow fiber membranes, while the relative abundance of both *Rehaibacterium* and *OCS116_clade* (*Rhizobiales*) decreased for flat sheet membranes. Overall, the NMDS plots of Bray-Curtis distances (Fig. S7, Supporting Information) indicated lower dissimilarity of bacterial community between the raw FPW and the biofouling layer of gravity-driven hollow fiber membranes than that between FPW and the biofouling layer of flat sheet membranes.

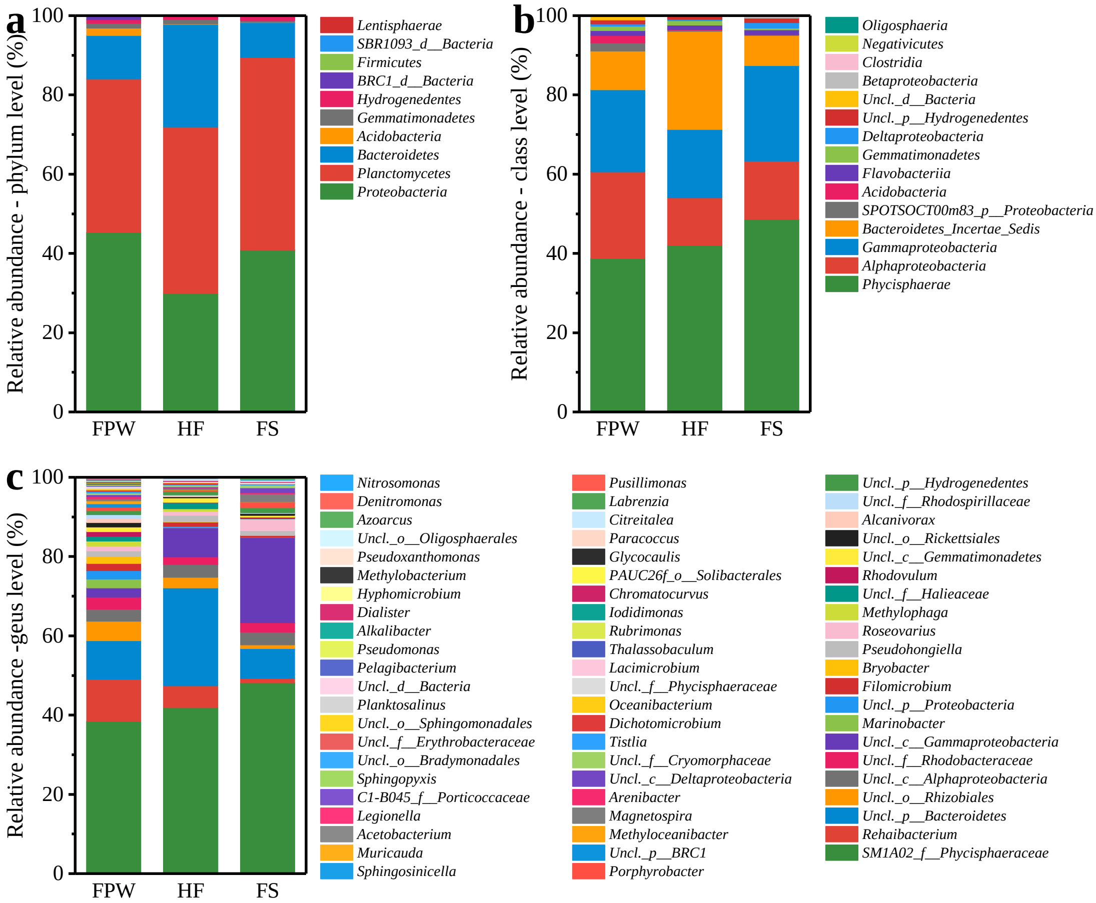

Fig. 4. Bacterial community compositions. Comparison of the bacterial communities in the raw FPW and in the biofouling layers of hollow fiber and flat sheet GDMs classified at (a) the phylum level, (b) the class level and (c) the genus level. FPW, HF and FS are abbreviations for raw shale gas FPW, GDM filtration using hollow fiber membrane, and GDM filtration using flat sheet membrane, respectively.

3.4.2. Eukaryotic community of the biofouling layer in GDM and comparison with the raw FPW

As presented in Fig. 5, the vastly predominant eukaryotic phyla in the raw shale gas FPW were *Ciliophora* (99.46%) in the kingdom of *Alveolata*. At the genus level, *Uronemella* in the class of *Intramacronucleata* represented the near totality of eukaryotes in the raw FPW. As listed in Table 1, both higher richness and diversity of eukaryotes were observed in the biofouling layer of GDMs compared to the raw shale gas FPW, especially for the flat sheet membranes. This result is evidenced by the increased number of classes or genera, from 8 in the raw shale gas FPW to 15 and 29 in GDM biofouling layer using hollow fiber membranes and flat sheet membranes, respectively (Figs. 5c-d). The Bray-Curtis distances (Fig. S7, Supporting Information) revealed lower dissimilarity between the raw FPW and biofouling layer in hollow fiber GDMs (0.10) than that between raw FPW and biofouling layer in flat sheet GDMs (0.16), and these values were much lower than those observed for the bacterial community (0.27-0.37).

More specifically, the relative abundance of fungi increased significantly in the biofouling layer for both membrane configurations. Additionally, other eukaryotic phyla, including *Ochrophyta*, unclassified *Eukaryota*, *Cnidaria*, *Florideophycidae*, *Porifera*, unclassified *Alveolata* (kingdom), and unclassified *Cryptophyceae* (kingdom), were found in the biofouling layer of gravity-driven flat sheet membranes (Fig. 5b). Most of these fungal communities were also previously reported in shale gas produced water from Sichuan Basin [29]. However, the kingdoms *Alveolata* and *Stramenopiles* were detected for the first time in shale gas FPW in this study. *Metazoa* were also detected on flat sheet membranes (Fig. 5). The high abundance of these latter organisms was previously reported in the GDM filtration of surface water and seawater [12,16,46]. The predation by eukaryotic microorganisms is a key factor influencing the biofouling layer structure of GDMs, resulting in a heterogeneous structure and thus a higher steady-state flux than that observed without eukaryotic predation, as discussed in the literature [12,46].

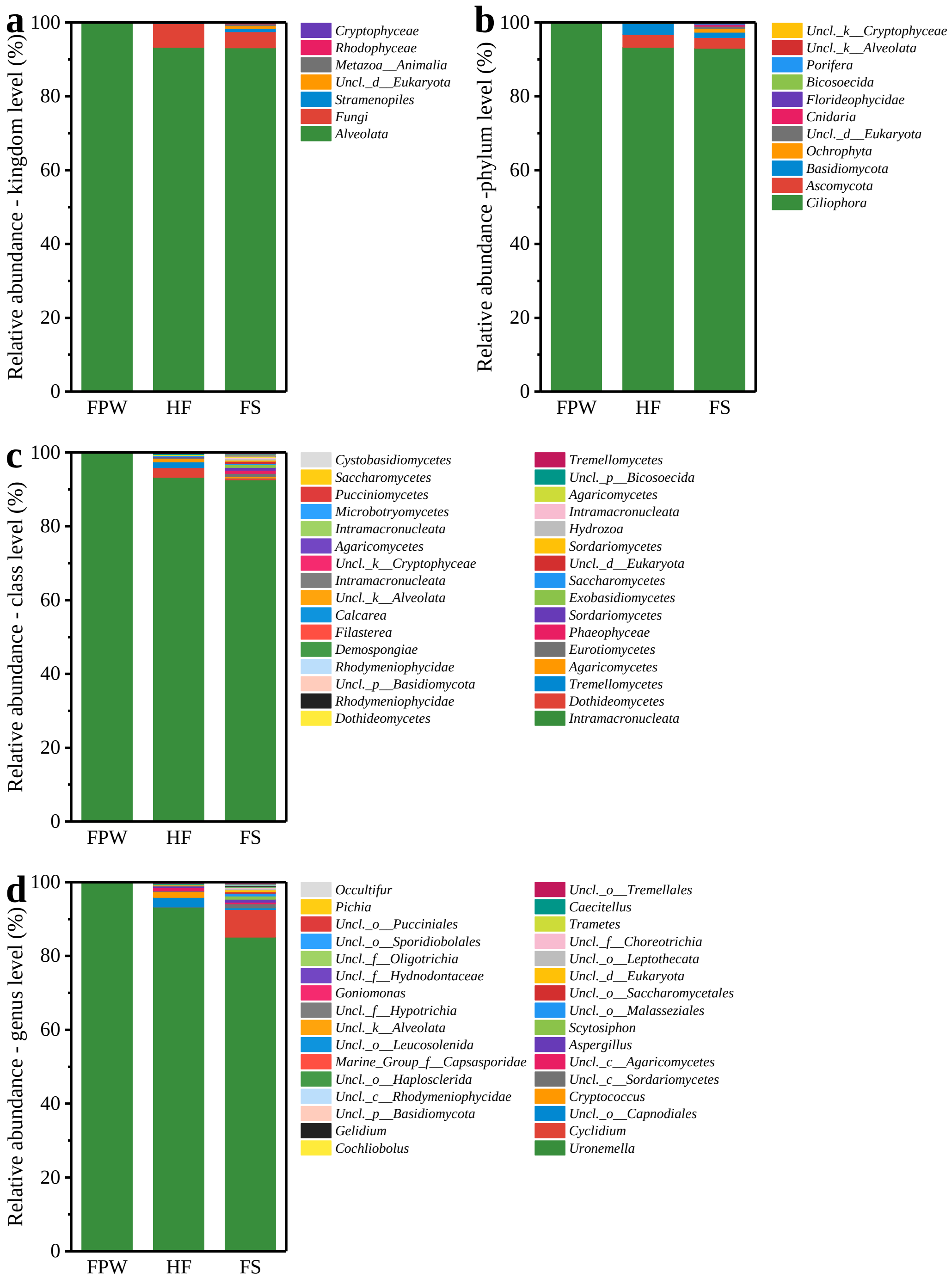

Fig. 5. Eukaryotic community compositions. Comparison of the Eukaryotic communities in the raw FPW and in the biofouling layers of hollow fiber and flat sheet GDMs classified at (a) the kingdom level, (b) the phylum level, (c) the class level and

(d) the genus level. The abbreviations FPW, HF and FS are the same as in Fig. 4.

3.5. Evaluation of GDM filtration performance for shale gas FPW treatment

3.5.1. Effect of GDM on desalination performance of NF and RO membranes

The SDI_{15} value of the permeate stream from traditional UF was 2.6±0.5, similar to that measured downstream of GDM filtrations. No significant difference was detected in the SDI_{15} of the permeates from GDMs operated at different pressure heads ($p > 0.05$), while a slightly higher SDI_{15} value was observed downstream of flat sheet gravity-driven membranes compared to hollow fiber membranes. In all the cases, the SDI_{15} was lower than 3.0, thus appropriate for an effective RO/NF desalination. Moreover, the consistency of flux decline behavior (Fig. 1) with the flow rate of shale gas FPW [3,4,7], further confirmed the sweet spot of GDM for this wastewater treatment.

To evaluate the potential of GDM filtration as a pretreatment for FPW desalination, the performance of NF/RO was evaluated using feed solutions from this system or from traditional UF (Fig. 6). Specifically, the mixture of the permeates obtained during the first year of operation of GDM using hollow fiber membranes under different pressure heads (H = 0.4, 0.8, 1.2 and 1.6 m) was fed to the NF/RO membranes; this mixed water was used because there was not a significant difference between the primary water parameters (e.g., TDS, EC, DOC, COD, turbidity, alkalinity and SDI_{15}) among these permeates, as presented in Fig. 3 and Fig. 6a.

During the filtration of FPW, the DOC concentrations of GDM permeate and UF permeate streams were comparable in this study, but the compositions of the DOC may be different. The excitation-emission matrix (EEM) spectra showed that aromatic protein, tyrosine- and protein-like substances were the primary fluorescent substances in raw shale gas FPW [36,58,59]. Additionally, liquid chromatography–organic carbon detection analysis indicated that biopolymers, humic substances, building blocks, low molecular weight (LMW) neutrals or LMW acids composed most of the DOC [58-60]. The removal of several organic fractions (e.g., biopolymers and assimilable organic carbon) in the GDM process was significantly higher than that by the traditional UF membrane, whereas more humic acids were rejected by the traditional UF membrane [10]. The different organic compounds resulted in different removals by the subsequent NF or RO units. Similar correlations were obtained in the filtration of seawater [16]. The superiority of GDM over traditional UF as NF pretreatment in organic removals is possibly due to the lower concentration of biopolymers assimilable organic carbon in the permeate stream, as demonstrated by Wu et al. [16]. Moreover, the pH values of the GDM permeate (Fig. 3h) were slightly higher than that of the UF permeate (~8.0) [34], and a higher DOC removal during nanofiltration of hydraulic fracturing wastewater with the increase in pH has been reported [61]. Thus, the overall organic removal efficiency (i.e., UV_{254} and DOC) of the NF membrane was improved when the GDM permeate was used as the feed water ($p < 0.05$), as presented in Fig. 6b. Also, the removal of TDS and EC in NF was slightly larger when treating GDM compared to UF permeate. On the other hand, the higher proportion of bicarbonate in the GDM permeate led to a lower removal of alkalinity in the following NF unit. Although a high removal of bicarbonate by NF membrane was reported [62], the removal efficiency of monovalent ion (HCO_3^-) was less than that of divalent ion (CO_3^{2-}). With respect to membrane fouling, the NF fluxes following GDM pretreatment were slightly larger than that after UF pretreatment, with an increase of 1-5%, as shown in Fig. 6c.

In RO, higher removal rates of TDS, EC, DOC and alkalinity were observed when using GDM permeate as the feed compared to the traditional UF permeate ($p < 0.05$), while the removal of UV_{254} was comparable ($p > 0.05$). However, a higher RO flux was observed when treating the GDM permeate compared to the traditional UF-RO process (Fig. 6d). This increase (4-10%) is regarded as significant, also considering that the NF/RO unit was run in dead-end mode. The advantage of GDM to traditional UF as RO pretreatment was also reported in seawater desalination for a 10-day operation [16], and attributed to lower concentrations of assimilable organic carbon in the GDM permeate. The permeate flux of RO membranes could be further improved when the GDM permeate stream was treated using a granular activated carbon filter or NF membrane (data not shown), or when the operation mode was optimized (e.g., crossflow filtration).

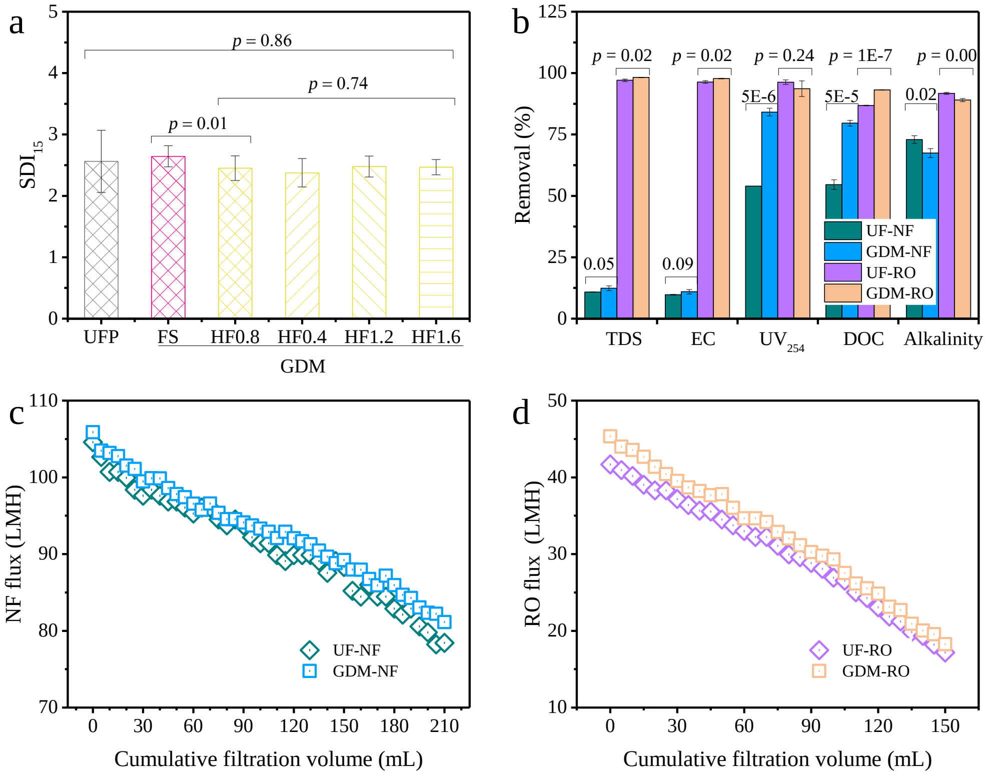

Fig. 6. Effect of GDM and traditional UF pretreatment on the desalination performance of NF and RO membranes: (a) SDI_{15} of the GDM permeate, (b) pollutant removals by NF/RO membrane treating GDM and traditional UF permeates, (c) flux decline in NF, and (d) flux decline in RO.

3.5.2. Application implications and outlook

Membrane technologies have potential application for the treatment and reuse of shale gas FPW [6]. For GDM systems, the permeate flux commonly decreases in the first several days of operation, before flux stabilization is obtained (Fig. 1). This flux decline trend is similar to the flowback rate of shale gas FPW (from 1,000 to 2-8 m^3/d) [3,7]. This implicates that the GDM filtration is suitable to also treat shale gas FPW in field applications. The flux stabilization of GDM systems was independent of membrane configuration or hydrostatic pressure. Thus, the similarities in performance observed for hollow fiber and flat sheet membranes suggest that the former configuration may be advantageous due to its larger specific surface area, thus translating into a smaller overall plant footprint. While the absolute values of steady-state flux are relatively low, they are justified by the nature of the driving force, a pressure head, which requires little external energy input to be maintained during filtration.

The pollutant removals of GDM systems (Figs. 3 and 6) showed their suitability for field application, and GDM filtration outperformed the traditional UF as pretreatment for the subsequent NF unit (increase by 1-5%) and RO unit (with an increase of 4-10%) (Fig. 6). As opposed to the cumbersome procedures (e.g., periodic backwashing or chemical cleaning [11]) of traditional UF process, the GDM system is an energy-efficient process due to the nature of the driving force, i.e., gravity. Thus, the energy demand of GDM system is in the order of 0.01 kWh/m^3 [10,63], depending on feed water characteristics. This value is significantly lower than the overall energy demand of conventional UF system (~0.3 kWh/m^3) [63,64]. On the other hand, the low flux is a potential limitation of GDM system, resulting in a larger footprint or a larger membrane area. For example, the steady-state flux of the GDM under a pressure head of 0.4 m (0.82 LMH) was less than 5% that of a conventional UF system (19 LMH, with a water recovery of 93%) observed during the filtration of shale gas FPW [33]. Thus, the membrane costs (investment and replacement) of GDM are higher than in traditional UF to produce the same volume of total permeate. Recently, Pronk et al. [10]

compared the total costs of GDM and traditional UF systems based on different scales. The stable flowback rate of shale gas FPW was 2-8 m^3/d per well [10]. Overall, the capital expenditure and membrane replacement costs for GDM and traditional UF systems depend very much on the specific conditions and on the size of the plant; however, the GDM system always had lower operational costs than the traditional UF process (i.e., chemical costs, energy costs, operation & maintenance), demonstrating that GDM may be attractive for FPW treatment under several circumstances..

Moreover, further studies to optimize the GDM system may address operational optimization, including length and parameters of filtration and washing cycles, with the goal to maintain high fluxes and to decrease membrane investment costs. Importantly, understanding the nature of the biofouling layer is critical for investigations aimed at minimizing fouling and optimizing filtration and cleaning cycles.

4 Conclusion

The performance of GDM filtration as pretreatment for the desalination of shale gas FPW was evaluated over a 612-day operation. The following conclusions can be drawn:

(1) The flux stabilization of GDM systems was independent of membrane configuration or hydrostatic pressure, and the steady-state values were in the range 0.65-0.82 L $m^{-2}h^{-1}$. The resistance associated to reversible fouling accounted for more than 89% of the total hydraulic resistance. While the absolute values of steady-state flux are relatively low, they are justified by the nature of the driving force, a pressure head, which requires little external energy input to be maintained during filtration.

(2) There was not a significant difference in the removal of TDS, organics, turbidity and alkalinity for the different GDM systems. The GDM filtration outperformed traditional UF as a desalination pretreatment, resulting in higher organic removal efficiencies and improved flux, especially for the RO system. While GDM filtration also relies on UF membranes for the aqueous separation, there are several advantages compared to traditional UF, including the absence of backwashing, cross-flow, and chemical cleaning. Overall, this translates into a substantial gain in terms of ease of operation and economic savings.

(3) The raw shale gas FPW contained more than 60 bacterial genera, with *SM1A02* and *Rehaibacterium* representing approximately half of the total genera. Eukaryotic communities in the kingdoms of *Alveolata* and *Stramenopiles* were detected for the first time in shale gas FPW.

(4) The bacterial community diversity decreased while the eukaryotic community diversity increased in the biofouling layer of GDMs, when compared to those of raw shale gas FPW. The predation by eukaryotic microorganisms including *Alveolata*, *Fungi*, *Stramenopiles* and *Metazoa* played an important role in flux stabilization during GDM filtration. Understanding the nature of the biofouling layer is critical for investigations aimed at minimizing fouling and optimizing filtration and cleaning cycles.

(5) For a long-term exposure, the variations of membrane permeability and contact angle were less significant than those related to elongation and tensile strength of the membranes. On the whole, long-term exposure to highly contaminated streams seems

to have no significant detrimental effect on system performance.

Acknowledgements

The work was supported by the National Natural Science Foundation of China (51708371, 51678377), China Postdoctoral Science Foundation (2018T110973, 2017M612965), the Applied Basic Research of Sichuan Province (2017JY0238), Sichuan University Outstanding Youth Foundation (2015SCU04A35), and Full-time Postdoctoral Foundation of Sichuan University (2017SCU12019). Alberto Tiraferri ackwnowledges the support of Compagnia di San Paolo and Politecnico di Torino through the project FLOWING. The authors thank Yi He, Qidong Wu, and Wancen Xie for SEM measurements.

Appendix A. Supplementary data

Supplementary data related to this article can be found online.

Reference

[1] A. Kondash, A. Vengosh, Water footprint of hydraulic fracturing, Environmental Science & Technology Letters, 2 (2015) 276-280.

[2] M. Yu, E. Weinthal, D. Patin˜o-Echeverri, M.A. Deshusses, C. Zou, Y. Ni, A. Vengosh, Water availability for shale gas development in Sichuan Basin, China, Environ. Sci. Technol., 50 (2016) 2837-2845.

[3] K.B. Gregory, R.D. Vidic, D.A. Dzombak, Water management challenges associated with the production of shale gas by hydraulic fracturing, Elements, 7 (2011) 181-186.

[4] R.D. Vidic, S.L. Brantley, J.M. Vandenbossche, D. Yoxtheimer, J.D. Abad, Impact of shale gas development on regional water quality, Science, 340 (2013) 1235009.

[5] D.L. Shaffer, L.H.A. Chavez, M. Ben-Sasson, S.R.-V. Castrillo´n, N.Y. Yip, M. Elimelech, Desalination and reuse of high-salinity shale gas produced water: drivers, technologies, and future directions, Environ. Sci. Technol., 47 (2013) 9569-9583.

[6] H. Chang, T. Li, B. Liu, R.D. Vidic, M. Elimelech, J.C. Crittenden, Potential and implemented

membrane-based technologies for the treatment and reuse of flowback and produced water from shale gas and oil plays: A review, Desalination, 455 (2019) 34-57.

[7] J.M. Estrada, R. Bhamidimarri, A review of the issues and treatment options for wastewater from shale gas extraction by hydraulic fracturing, Fuel, 182 (2016) 292-303.

[8] S.M. Riley, J.M.S. Oliveira, J. Regnery, T.Y. Cath, Hybrid membrane bio-systems for sustainable treatment of oil and gas produced water and fracturing flowback water, Sep. Purif. Technol., 171 (2016) 297-311.

[9] M. Tawalbeh, A.A. Mojjly, A. Al-Othman, N. Hilal, Membrane separation as a pre-treatment process for oily saline water, Desalination, 447 (2018) 182–202.

[10] W. Pronk, A. Ding, E. Morgenroth, N. Derlon, P. Desmond, M. Burkhardt, B. Wu, A.G. Fane, Gravity-driven Membrane Filtration for Water and Wastewater Treatment: A Review, Water Res., 149 (2019) 553-565.

[11] M. Peter-Varbanets, F. Hammes, M. Vital, W. Pronk, Stabilization of flux during dead-end ultra-low pressure ultrafiltration, Water Res., 44 (2010) 3607-3616.

[12] N. Derlon, M. Peter-Varbanets, A. Scheidegger, W. Pronk, E. Morgenroth, Predation influences the structure of biofilm developed on ultrafiltration membranes, Water Res., 46 (2012) 3323-3333.

[13] E. Akhondi, B. Wu, S. Sun, B. Marxer, W. Lim, J. Gu, L. Liu, M. Burkhardt, D. McDougald, W. Pronk, A.G. Fane, Gravity-driven membrane filtration as pretreatment for seawater reverse osmosis: Linking biofouling layer morphology with flux stabilization, Water Res., 70 (2015) 158-173.

[14] B. Wu, F. Hochstrasser, E. Akhondi, N. Ambauen, L. Tschirren, M. Burkhardt, A.G. Fane, W. Pronk, Optimization of gravity-driven membrane (GDM) filtration process for seawater pretreatment, Water Res., 93 (2016) 133-140.

[15] B. Wu, T. Christen, H.S. Tan, F. Hochstrasser, S.R. Suwarno, X. Liu, T.H. Chong, M. Burkhardt, W. Pronk, A.G. Fane, Improved performance of gravity-driven membrane filtration for seawater pretreatment: Implications of membrane module configuration, Water Res., 114 (2017) 59-68.

[16] B. Wu, S.R. Suwarno, H.S. Tan, L.H. Kim, F. Hochstrasser, T.H. Chong, M. Burkhardt, W. Pronk, A.G. Fane, Gravity-driven microfiltration pretreatment for reverse osmosis (RO) seawater desalination: Microbial community characterization and RO performance, Desalination, 418 (2017) 1-8.

[17] B. Kus, J. Kandasamy, S. Vigneswaran, H. Shon, G. Moody, Gravity driven membrane filtration system to improve the water quality in rainwater tanks, Water Sci. Technol. Water Supply, 13 (2013) 479-485.

[18] X. Tang, A. Ding, F. Qu, R. Jia, H. Chang, X. Cheng, B. Liu, G. Li, H. Liang, Effect of operation parameters on the flux stabilization of gravity-driven membrane (GDM) filtration system for decentralized water supply, Environmental Science and Pollution Research, 23 (2016) 16771-16780.

[19] M. Peter-Varbanets, J. Margot, J. Traber, W. Pronk, Mechanisms of membrane fouling during ultra-low pressure ultrafiltration, J. Membr. Sci., 377 (2011) 42-53.

[20] N. Derlon, N. Koch, B. Eugster, T. Posch, J. Pernthaler, W. Pronk, E. Morgenroth, Activity of metazoa governs biofilm structure formation and enhances permeate flux during Gravity-Driven Membrane (GDM) filtration, Water Res., 47 (2013) 2085-2095.

[21] G.A. Kahrilas, J. Blotevogel, P.S. Stewart, T. Borch, Biocides in hydraulic fracturing fluids: A critical review of their usage, mobility, degradation, and toxicity, Environ. Sci. Technol., 49 (2015) 16-32.

[22] M.K. Camarillo, J.K. Domen, W.T. Stringfellow, Physical-chemical evaluation of hydraulic fracturing chemicals in the context of produced water treatment, J. Environ. Manage., 183 (2016) 164-174.
[23] C.G. Struchtemeyer, M.S. Elshahed, Bacterial communities associated with hydraulic fracturing fluids in thermogenic natural gas wells in North Central Texas, USA, FEMS Microbiol. Ecol., 81 (2012) 13-25.
[24] P.J. Mouser, M. Borton, T.H. Darrah, A. Hartsock, K.C. Wrighton, Hydraulic fracturing offers view of microbial life in the deep terrestrial subsurface, FEMS Microbiol. Ecol., 92 (2016) fiw166.
[25] D. Lipus, A. Vikram, D. Ross, D. Bain, D. Gulliver, R. Hammack, K. Bibby, Predominance and metabolic potential of Halanaerobium spp. in produced water from hydraulically fractured Marcellus shale wells, Appl. Environ. Microbiol., 83 (2017) e02659-02616.
[26] A. Murali Mohan, A. Hartsock, R.W. Hammack, R.D. Vidic, K.B. Gregory, Microbial communities in flowback water impoundments from hydraulic fracturing for recovery of shale gas, FEMS Microbiol. Ecol., 86 (2013) 567-580.
[27] C. Wuchter, E. Banning, T.J. Mincer, N.J. Drenzek, M.J. Coolen, Microbial diversity and methanogenic activity of Antrim Shale formation waters from recently fractured wells, Frontiers in microbiology, 4 (2013) 367.
[28] R.A. Daly, M.A. Borton, M.J. Wilkins, D.W. Hoyt, D.J. Kountz, R.A. Wolfe, S.A. Welch, D.N. Marcus, R.V. Trexler, J.D. MacRae, J.A. Krzycki, D.R. Cole, P.J. Mouser, K.C. Wrighton, Microbial metabolisms in a 2.5-km-deep ecosystem created by hydraulic fracturing in shales, Nature microbiology, 1 (2016) 16146.
[29] Y. Zhang, Z. Yu, H. Zhang, I.P. Thompson, Microbial distribution and variation in produced water from separators to storage tanks of shale gas wells in Sichuan Basin, China, Environmental Science: Water Research & Technology, 3 (2017) 340-351.
[30] M.A. Cluff, A. Hartsock, J.D. MacRae, K. Carter, P.J. Mouser, Temporal changes in microbial ecology and geochemistry in produced water from hydraulically fractured Marcellus shale gas wells, Environ. Sci. Technol., 48 (2014) 6508-6517.
[31] V.B. Frank, J. Regnery, K.E. Chan, D.F. Ramey, J.R. Spear, T.Y. Cath, Co-treatment of residential and oil and gas production wastewater with a hybrid sequencing batch reactor-membrane bioreactor process, Journal of Water Process Engineering, 17 (2017) 82-94.
[32] T.L.S. Silva, S. Morales-Torres, S. Castro-Silva, J.L. Figueiredo, A.M.T. Silva, An overview on exploration and environmental impact of unconventional gas sources and treatment options for produced water, J. Environ. Manage., 200 (2017) 511-529.
[33] C. Guo, H. Chang, B. Liu, Q. He, B. Xiong, M. Kumar, A.L. Zydney, An ultrafiltration- reverse osmosis combined process for external reuse of Weiyuan shale gas flowback and produced water, Environmental Science: Water Research & Technology, 4 (2018) 942-955.
[34] H. Chang, B. Liu, B. Yang, X. Yang, C. Guo, Q. He, S. Liang, S. Chen, P. Yang, An integrated coagulation-ultrafiltration-nanofiltration process for internal reuse of shale gas flowback and produced water, Sep. Purif. Technol., 211 (2019) 310-321.
[35] A. International, Standard Test Method for Silt Density Index (SDI) of Water, in, West Conshohocken, PA, 2014.
[36] H. Chang, T. Li, B. Liu, C. Chen, Q. He, J.C. Crittenden, Smart ultrafiltration membrane fouling control as desalination pretreatment of shale gas fracturing wastewater: The effects of backwash water, Environ. Int., (2019).

[37] G.K. Batchelor, An Introductionto Fluid Dynamics, Cambridge University Press, Cambridge, 2000.
[38] S. Shao, Y. Feng, H. Yu, J. Li, G. Li, H. Liang, Presence of an adsorbent cake layer improves the performance of gravity-driven membrane (GDM) filtration system, Water Res., 108 (2017) 240-249.
[39] X. Tang, W. Pronk, A. Ding, X. Cheng, J. Wang, B. Xie, G. Li, H. Liang, Coupling GAC to ultra-low-pressure filtration to modify the biofouling layer and bio-community: Flux enhancement and water quality improvement, Chem. Eng. J., 333 (2018) 289-299.
[40] S. Shao, D. Shi, Y. Li, Y. Liu, Z. Lu, Z. Fang, H. Liang, Effects of water temperature and light intensity on the performance of gravity-driven membrane system, Chemosphere, 216 (2019) 324-330.
[41] U.S.E.P.A.O.o. Water, Membrane filtration guidance manual, United States Environmental Protection Agency, Office of Water, 2005.
[42] A. Ding, H. Liang, G. Li, N. Derlon, I. Szivak, E. Morgenroth, W. Pronk, Impact of aeration shear stress on permeate flux and fouling layer properties in a low pressure membrane bioreactor for the treatment of grey water, J. Membr. Sci., 510 (2016) 382-390.
[43] R.I. Griffiths, A.S. Whiteley, A.G. O'Donnell, M.J. Bailey, Rapid method for coextraction of DNA and RNA from natural environments for analysis of ribosomal DNA- and rRNA-based microbial community composition, Appl. Environ. Microbiol., 66 (2000) 5488-5491.
[44] X. Zhang, D. Zhang, Y. Huang, K. Zhang, P. Lu, Simultaneous removal of organic matter and iron from hydraulic fracturing flowback water through sulfur cycling in a microbial fuel cell, Water Res., 147 (2018) 461-471.
[45] N. Derlon, A. Grütter, F. Brandenberger, A. Sutter, U. Kuhlicke, T.R. Neu, E. Morgenroth, The composition and compression of biofilms developed on ultrafiltration membranes determine hydraulic biofilm resistance, Water Res., 102 (2016) 63-72.
[46] T. Klein, D. Zihlmann, N. Derlon, C. Isaacson, I. Szivak, D.G. Weissbrodt, W. Pronk, Biological control of biofilms on membranes by metazoans, Water Res., 88 (2016) 20-29.
[47] A. Ding, H. Liang, G. Li, I. Szivak, J. Traber, W. Pronk, A low energy gravity-driven membrane bioreactor system for grey water treatment: Permeability and removal performance of organics, J. Membr. Sci., 542 (2017) 408-417.
[48] A. Ding, J. Wang, D. Lin, X. Tang, X. Cheng, G. Li, N. Ren, H. Liang, In situ coagulation versus pre-coagulation for gravity-driven membrane bioreactor during decentralized sewage treatment: Permeability stabilization, fouling layer formation and biological activity, Water Res., 126 (2017) 197-207.
[49] A. Ding, J. Wang, D. Lin, X. Tang, X. Cheng, H. Wang, L. Bai, G. Li, H. Liang, A low pressure gravity-driven membrane filtration (GDM) system for rainwater recycling: Flux stabilization and removal performance, Chemosphere, 172 (2017) 21-28.
[50] Y. Wang, L. Fortunato, S. Jeong, T. Leiknes, Gravity-driven membrane system for secondary wastewater effluent treatment: Filtration performance and fouling characterization, Sep. Purif. Technol., 184 (2017) 26-33.
[51] B.D. Coday, C. Hoppe-Jones, D. Wandera, J. Shethji, J. Herron, K. Lampi, S.A. Snyder, T.Y. Cath, Evaluation of the transport parameters and physiochemical properties of forward osmosis membranes after treatment of produced water, J. Membr. Sci., 499 (2016) 491-502.
[52] M.F. Kirk, A.M. Martini, D.O. Breecker, D.R. Colman, C. Takacs-Vesbach, S.T. Petsch, Impact of

commercial natural gas production on geochemistry and microbiology in a shale-gas reservoir, Chem. Geol., 332-333 (2012) 15-25.

[53] B. Akyon, E. Stachler, Na Wei, K. Bibby, Microbial mats as a biological treatment approach for saline wastewaters: The case of produced water from hydraulic fracturing, Environ. Sci. Technol., 49 (2015) 6172-6180.

[54] A. Murali Mohan, A. Hartsock, K.J. Bibby, R.W. Hammack, R.D. Vidic, K.B. Gregory, Microbial Community Changes in Hydraulic Fracturing Fluids and Produced Water from Shale Gas Extraction, Environ. Sci. Technol., 47 (2013) 13141-13150.

[55] N.M. Hull, J.S. Rosenblum, C.E. Robertson, J.K. Harris, K.G. Linden, Succession of toxicity and microbiota in hydraulic fracturing flowback and produced water in the Denver-Julesburg Basin, Sci. Total Environ., 644 (2018) 183-192.

[56] A. Vikram, D. Lipus, K. Bibby, Metatranscriptome analysis of active microbial communities in produced water samples from the Marcellus Shale, Microb. Ecol., 72 (2016) 571-581.

[57] K.J. Bibby, S.L. Brantley, D.D. Reible, K.G. Linden, P.J. Mouser, K.B. Gregory, B.R. Ellis, R.D. Vidic, Suggested reporting parameters for investigations of wastewater from unconventional shale gas extraction, Environ. Sci. Technol., 47 (2013) 13220-13221.

[58] F.-x. Kong, G.-d. Sun, J.-f. Chen, J.-d. Han, C.-m. Guo, Tong-Zhang, X.-f. Lin, Y.F. Xie, Desalination and fouling of NF/low pressure RO membrane for shale gas fracturing flowback water treatment, Sep. Purif. Technol., 195 (2018) 216-223.

[59] S.M. Riley, D.C. Ahoor, J. Regnery, T.Y. Cath, Tracking oil and gas wastewater-derived organic matter in a hybrid biofilter membrane treatment system: A multi-analytical approach, Sci. Total Environ., 613-614 (2018) 208-217.

[60] A. Butkovskyi, A.-H. Faber, Y. Wang, K. Grolle, R. Hofman-Caris, H. Bruning, A.P.V. Wezel, H.H.M. Rijnaarts, Removal of organic compounds from shale gas flowback water, Water Res., 138 (2018) 47-55.

[61] S.M. Dischinger, J. Rosenblum, R.D. Noble, D.L. Gin, K.G. Linden, Application of a lyotropic liquid crystal nanofiltration membrane for hydraulic fracturing flowback water: Selectivity and implications for treatment, J. Membr. Sci., 543 (2017) 319-327.

[62] A.P. Padilla, H. Saitua, Performance of simultaneous arsenic, fluoride and alkalinity (bicarbonate) rejection by pilot-scale nanofiltration, Desalination, 257 (2010) 16-21.

[63] A.G. Fane, A grand challenge for membrane desalination: More water, less carbon, Desalination, 426 (2018) 155-163.

[64] G.K. Pearce, UF/MF pre-treatment to RO in seawater and wastewater reuse applications: a comparison of energy costs, Desalination, 222 (2008) 66-73.